Nanostructure of a vicinal surface of $SrTiO_3$: Order on two length scales

Isabelle Joumard,[1,*] Xavier Torrelles,[2] Tien-Lin Lee,[1] Oier Bikondoa,[2] Jordi Rius,[2] and Jorg Zegenhagen[1]
[1]*European Synchrotron Radiation Facility, F-38043 Grenoble, France*
[2]*Institut de Ciència de Materials de Barcelona (CSIC), 08193 Bellaterra, Barcelona, Spain*
(Received 22 June 2006; revised manuscript received 15 September 2006; published 8 November 2006)

Grazing incidence x-ray diffraction, combined with low energy electron diffraction and scanning tunneling microscopy shows that annealed $SrTiO_3(103)$ surfaces exhibit regular nanostructures on two length scales with shorter (~1.2 nm) ripples bunching to longer (~7.4 nm) waves, corresponding to six $SrTiO_3(103)$ unit cells. The surface, wavy in the [100] direction, exhibits SrO and TiO_2 terminated "steps." Lateral relaxations along the [010] direction of the unit cell lead to a weak (1×2) reconstruction. Electrostatic forces are thought to be responsible for the observed surface morphology.

DOI: 10.1103/PhysRevB.74.205411 PACS number(s): 61.10.Eq, 61.14.Hg, 68.35.Bs, 68.37.Ef

I. INTRODUCTION

$SrTiO_3$ (STO) has been studied extensively because of its superconductivity,[1] catalytic- and photoactivity[2] and surface ferroelectricity.[3] It is also considered for applications as gas sensors[4] and dielectric with large permittivity in microelectronic applications.[5,6] In all cases, the STO surface structures play an important role. Furthermore, knowing and controlling the surface properties of $SrTiO_3$ is a prerequisite for its utilization as substrate for growing epitaxial giant magnetoresistance[7] and high temperature superconductor (HTS) materials.[8] For instance stepped STO(106) substrate surfaces can be used to create effectively flux pinning centers in HTS thin films, permitting exceptionally high critical currents.[9] Moreover, some regular nanoscale patterns created by strain relief or reconstruction may serve as templates to define the pattern of nanostructures upon heteroepitaxial growth.

In spite of these rich properties and important applications, mainly due to the complexity of the structures, STO surfaces are by far less well understood compared to their metal or semiconductor counterparts. Primarily the (001) (Refs. 8 and 10) but also the (110) (Ref. 11) and less intensively the (111) (Ref. 8) surfaces of STO have been studied and found to exhibit a large number of reconstructions. Typical for an insulator with strong ionic bonds, some orientations of STO [(110) and (111)] are characterized as polar surfaces. The electronic instability resulting from the presence of macroscopic dipoles due to some peculiar orientations, can only be canceled by the introduction of compensating charges in the outer planes. This can be achieved either by modification of the surface electronic structure, by faceting or reconstruction, or by changes in the surface stoichiometry.[12] The electronic and atomic structure will of course depend on the surface preparation conditions.

Diffraction techniques represent a powerful tool for solving surface structures and refining atomic positions even in the case of large scale reconstructions. We recently solved the structure of $SrTiO_3(106)$ by grazing incidence x-ray diffraction (GIXRD) and direct methods[13] supported by scanning tunneling microscopy (STM) and low energy electron diffraction (LEED) data. The surface exhibits SrO and TiO_2 terminated unstrained half-steps with the surface atoms being practically in their bulklike positions. The resulting wavy surface reveals an astonishing degree of long-range order, which is thought to be established by the alternating, weakly polar surface terminations. Since cation sites are only partially occupied toward step edges, the overall corrugation is diminished but the surface lacks short-range order. This is very different from the behavior observed for metal and semiconductor surfaces, where stress resulting from short-range reconstruction is the driving force behind long-range order.

II. EXPERIMENT

The surface of our STO sample crystal was cut with an accuracy better than 0.1° parallel to the (103) plane and polished to an optical finish. It was loaded into a multichamber ultrahigh vacuum (UHV) system and then annealed at slowly increasing temperatures up to 1000 °C, keeping the pressure in the 10^{-10} mbar range. It had been proven that for STO annealing alone, in UVH or clean oxygen, is sufficient to produce clean and long range ordered surfaces.[8] Several stable reconstructions or superstructures induced by oxygen vacancies after UHV annealing have been previously observed by STM measurements on $SrTiO_3(001)$ surfaces by different groups:[14–16] 1×1, 2×1, 2×2, $c(4\times2)$, $c(4\times4)$, and $c(6\times2)$. The sample was then cooled down for LEED and STM measurements carried out at room temperature. UHV annealing gives rise to oxygen vacancies in the STO bulk, inducing sufficient conductivity for LEED and STM measurements. Several annealing cycles, each lasting about 10 hours, have been necessary to produce a clean and well ordered surface as shown by LEED and STM (Fig. 1).

For the structural analysis and refinement, we used a tetragonal (103) surface unit cell [side view shown in Fig. 2(a)], which is described by

$$\mathbf{a_X} = \left[\frac{3 * a_{\mathrm{STO}}}{\cos\Theta}, 0, 0\right],$$

$$\mathbf{a_Y} = [0, a_{\mathrm{STO}}, 0],$$

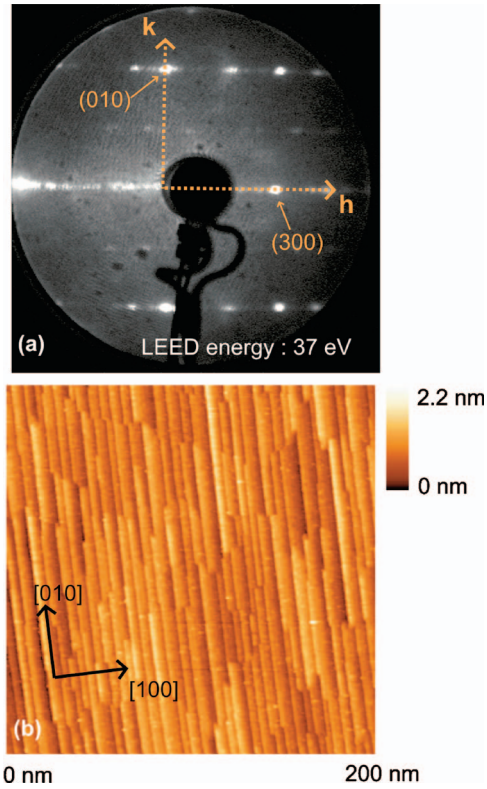

FIG. 1. (Color)(a) LEED pattern and (b) STM topography of the $SrTiO_3$(103) vicinal surface. The STM image show a wavy modulation along [100] direction.

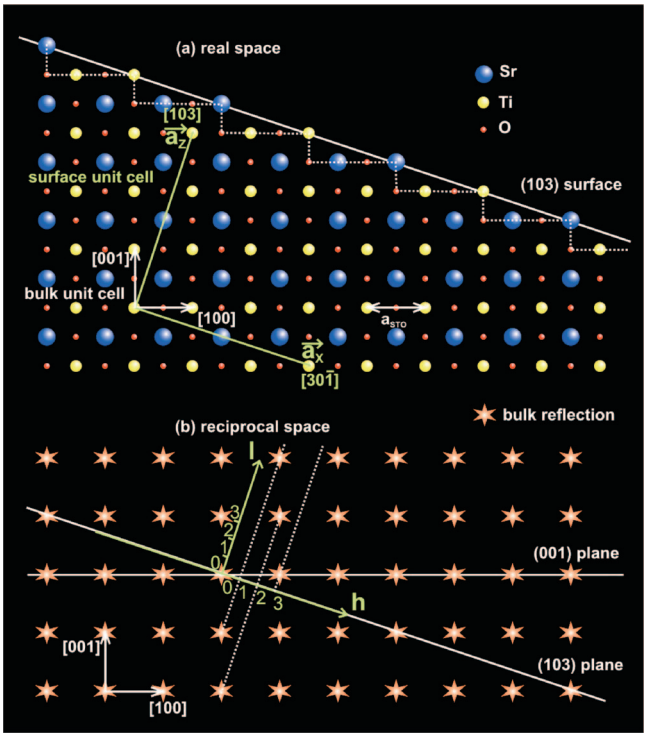

FIG. 2. (Color) Side view of the bulk and surface unit cells (a) in the real space and (b) in the reciprocal space. In the part (a) of the figure, the dotted line follows the expected (103) surface deduced from our previous results on the (106) surface. In the part (b) of the figure, the white dotted lines indicate the expected CTRs.

$$\mathbf{a_Z} = \left[0,0,\frac{3 * a_{STO}}{\cos\Theta}\right],$$

where a_{STO}=3.905 Å, $\alpha=\beta=\gamma=90°$, and $\Theta=\tan^{-1}(1/3)$. This coordinate system is thus chosen with the X, Y, and Z axes parallel to the bulk STO [30$\bar{1}$], [010], and [103] directions, respectively.

From the previous results obtained for the STO(106) surface,[13] the STO(103) surface is expected to exhibit a structure which is schematically shown in the upper part of Fig. 2. This is a steplike structure with "terraces" between steps parallel to the bulk [100] direction being alternatively Sr and Ti terminated. The expected size of the terraces along the [100] direction should be 1.5 times the bulk lattice parameter a_{STO}.

III. RESULTS

A. Leed and STM results

In the LEED pattern of STO(103) shown in Fig. 1(a), the first Brillouin zone, i.e., the reciprocal lattice unit cell of the (103)STO surface unit cell is spanned in the h and k direction by the [100] and [010] reflections, respectively. In the h direction the third order reflections ($3*n$) (where n is an integer) are well defined whereas the other reflections, which are also due to crystal truncation rods (CTRs) and indicate a very smooth (103) surface, are less clear. The position of these spots is not well defined, but between $3*n/2$ and $2*n$, suggesting that the (103) surface described in Fig. 2 may not be the real optical surface probed by the electrons. Furthermore, at the chosen LEED energy of 37 eV, streaks of reflected intensity can be distinguished at $k=\pm 1/2$, indicating a twofold periodicity in the k direction, which is along the step edges in the STM image in Fig. 1(b). This STM image shows a regular "terrace" structure with edges along the [010] direction. The periodicity of this wavy pattern of the surface is about 7 nm in average, which is the length of about six STO(103) surface cells. The overall appearance of the surface is quite similar to the STO(106) surface, where STM and LEED investigations revealed a morphology on the nanoscale which had been described as a regular "step structure."[17] Higher resolution STM images of the (103) surface (shown in Fig. 3) cannot reveal any superstructure along the step edges, i.e., the [010] direction. Similar to the observations reported for the STO(106) surface,[13] many contrast variations can be distinguished along the [100] direction. Line profiles of the STM image show sharp step features (1.2 nm in length) corresponding to the size of one (103) surface unit cell.

B. GIXRD results

To solve the structure of the STO(103) surface we used GIXRD at the insertion device beamline ID32 of the European Synchrotron Radiation Facility (ESRF). A sample prepared and characterized in the above described way was transferred into a portable UHV chamber without breaking

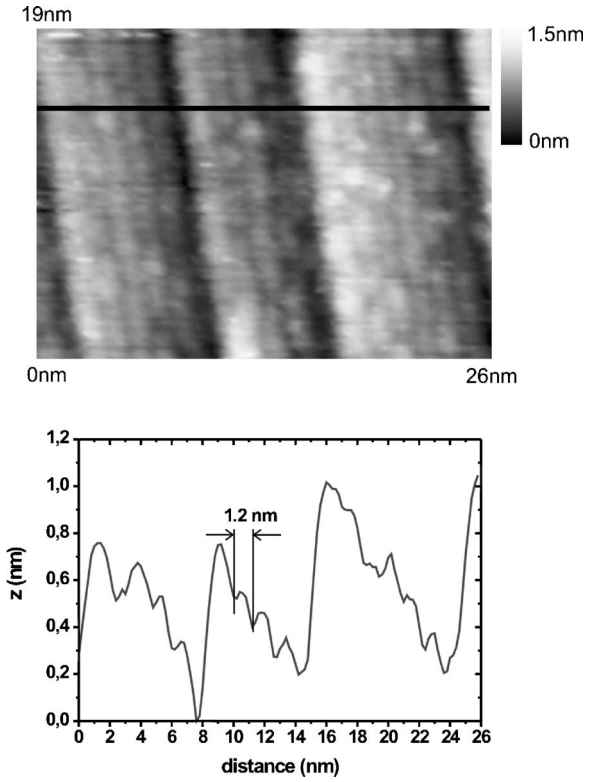

FIG. 3. High resolution STM image of the $SrTiO_3$(103) vicinal surface. The line profile taken along the black line on the STM image shows small modulations (1.2 nm length) between two steps in the [100] direction.

the UHV. The portable chamber was then mounted on the six-circle diffractometer at the ID32 beamline. The incident angle of the 15 keV x rays with respect to the sample surface was selected close to the critical angle (Θ_c=0.25°). Integrated intensities were recorded for 26 CTRs and six half-order rods. The number of the half-order rods which could be measured was limited due to some roughness of the surface. The total number of the nonequivalent reflections was 1636.

The long-range order of the surface was inferred from the angular widths $\triangle h$ and $\triangle k$ (FWHM) of the integer order reflections recorded at grazing exit angles, i.e., with negligible perpendicular momentum transfer. From the widths of several reflections, the domain size was determined to be around 130 nm along the steps edges and close to 8 nm in the perpendicular direction, which corresponds to the average periodicity of the surface modulation observed by STM in Fig. 1(b).

To analyze the data, we used the ROD program,[18] which allows fitting the parameters of a chosen structural model to the data and minimizing χ^2. As the first structural model, we used an ideal STO(103)-(1×1) surface cell termination and considered only the CTRs data. It was not possible to fit the experimental data by allowing only atomic relaxations (in-plane as well as out-of-the-surface plane). Occupancies O_c smaller than unity for the atomic sites of the surface atoms must be assumed and play a fundamental role. Other fitting parameters like Debye-Waller factors were tested but did not improve significantly the agreement between the data and the

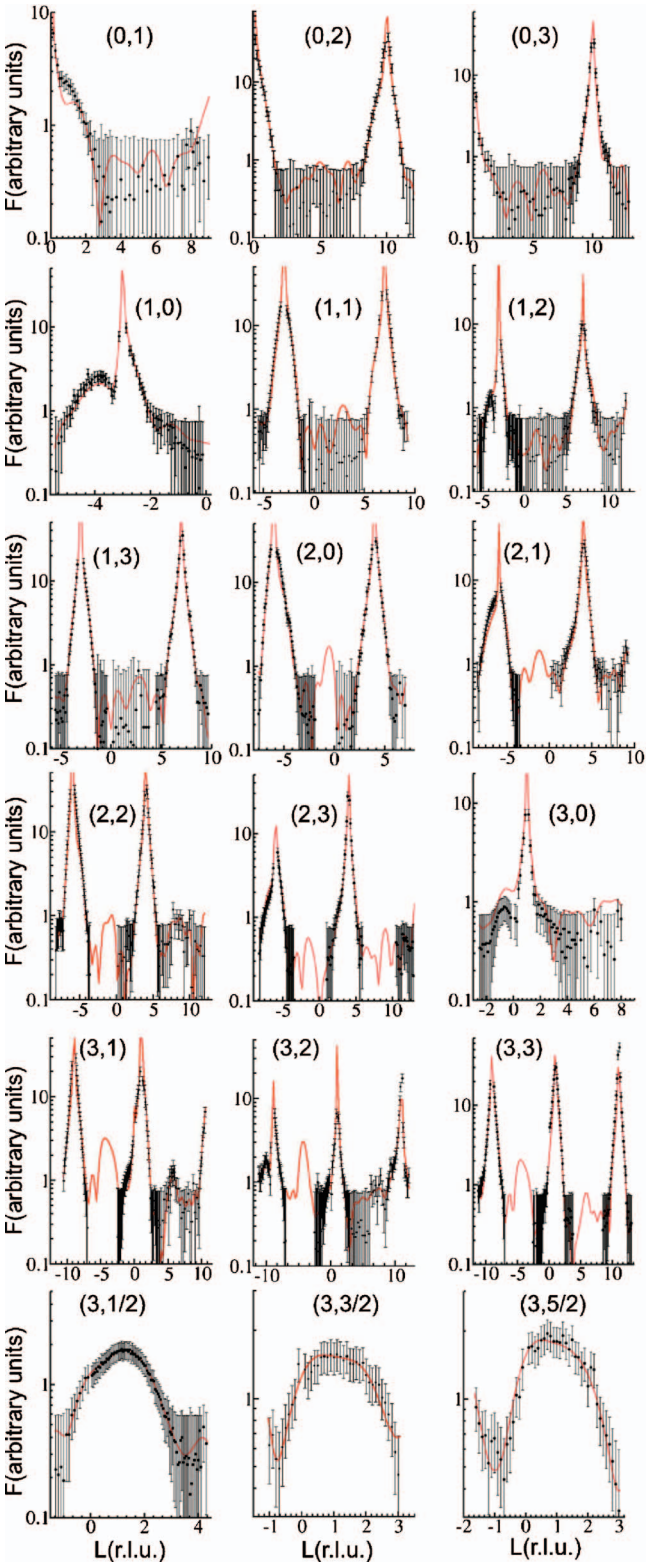

FIG. 4. (Color) Several representative crystal truncation rods and fractional order rods (last bottom line). Calculated (red line, from the structure displayed in Fig. 5) and measured structure factors (black symbols) are shown on a logarithmic scale. The size of the error bars appears exaggerated owing to their representation on a logarithmic scale. Error bars around the minimum of the CTR's can be as large as the structure factor values due to the unfavorable signal to noise ratio in these regions.

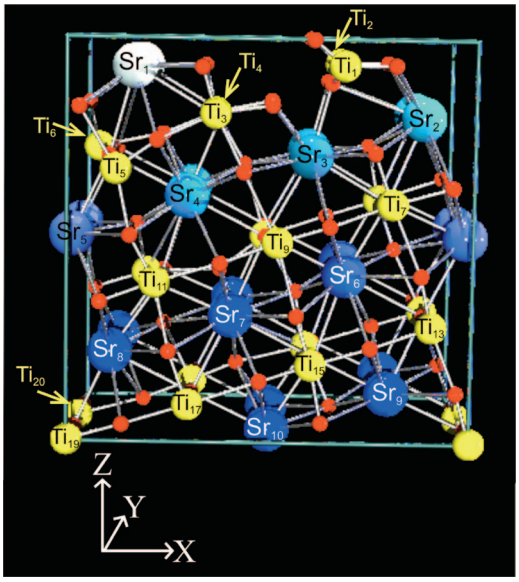

FIG. 5. (Color) Lateral view of the $SrTiO_3(103)$-(1×2) superstructure according to the final refinement. The occupancies of the topmost Sr atomic sites are indicated by the intensity of the blue color. Lighter color means lower occupancy. For Ti atomic sites (in yellow) no occupancy indication is given. Maximum geometric distortions are observed for atomic sites with partial occupancies.

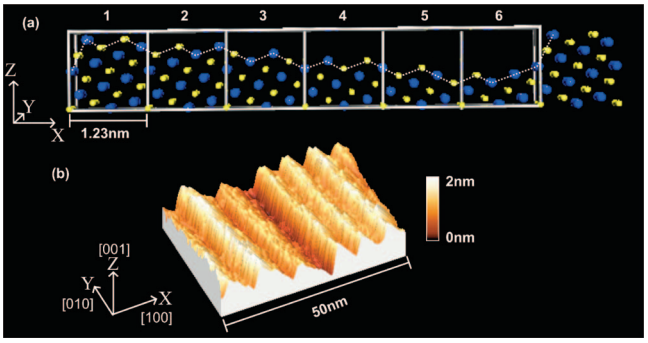

FIG. 6. (Color) (a) Structural model, which reconciles the partial population factors in the (103)-1×2 cell as obtained from the analysis of the X-ray data (cf. Fig. 5 and Table I) and the STM images. The partial occupancies of atomic sites in one $SrTiO_3(103)$-1×2 unit cell are equivalent to a SrTiO3(103)-6×2 supercell, where the individual (103)-1×2 cells are from one to six gradually only partially filled with atoms. For clarity, only the Sr (blue) and Ti (yellow) atoms are shown. The dotted line is a guide for the eyes indicating the surface terminations (b) 3D STM image showing the terrace structure with a periodicity of around 8 nm. The width of each terrace corresponds roughly to the length of one SrTiO3(103)-6×2 supercell.

fit. With relaxation along the X and Z directions and one single Debye-Waller factor included as free fitting parameters for all the atoms in the (103) unit cell, the result of the fit showed that O_c of Sr and Ti had a linear dependence on their Z coordinate, which can be described as (see Fig. 5)

$$O_c(\mathrm{Sr,Ti}) = (5/3) * (1 - Z) \quad \text{for } 0.4 \leqslant Z \leqslant 1.0,$$

$$O_c(\mathrm{Sr,Ti}) = 1 \quad \text{for } Z \leqslant 0.3.$$

In the second step, we included the measured half-order rods in the fitting by doubling the surface unit cell in the Y direction. The atoms in the new (1×2) supercell were allowed to move along the X, Y, and Z directions, restricted, however, by the experimentally observed *pm* symmetry. In the final refinement the occupancies of the cations were allowed to vary as well. The occupancies of the oxygen atoms were kept fixed to the nearest neighbor cation occupancy values (in case there was the choice between different values, the lowest occupancy was chosen for oxygen). With such a model considering 137 structural parameters (corresponding to degrees of freedom of Sr, Ti and O atoms) and 11 occupancy parameters, a fit goodness (χ^2) of about 1.4 is obtained. Figure 4 illustrates the good agreement between experimental and calculated rods obtained from the fitting procedure.

The maximum displacements are obtained for outermost surface atoms, but the error bars are here fairly large since their lower occupancy values reduce their weight in the fitting process. The ideal atomic coordinates of Sr and Ti atoms in the (1×2) surface cell, as well as their relative displacements obtained from the best fit are given in Table I and a view along the [010] direction of the resulting (1×2) structure is given in Fig. 5. Also listed in Table I are the occupancies of the different atomic sites, as well as cation-anion bond lengths resultant from the determined atomic positions.

As expected, the structural relaxation of the cations decreases with depth from the surface. In the Z direction, the Sr_1 atom is relaxed outwards by 2.8% whereas the others Sr_i $(i>1)$ are relaxed by less than 0.3%. Concerning the Ti atoms, Ti_1 and Ti_2 are relaxed outwards by 3.7%. The Z relaxation for Ti atoms becomes practically negligible for the Ti atoms located in the bottom half cell.

The (1×2) periodicity is caused by lateral atomic movements along the X direction of Ti atoms (Ti_5 to Ti_{12} in Table I) located on the mirror planes $(X,0)$ and $(X,1/2)$ in the (1×2) unit cell. The relative displacements along the X direction of the Ti_5, Ti_7, Ti_9, and Ti_{11} atoms located in the $(X,0)$ plane are significant and opposite to the relative displacements of the Ti_6, Ti_8, Ti_{10}, and Ti_{12} atoms located in the $(X,1/2)$ plane. However, displacements of Ti_5 and Ti_6 atoms exhibit a fairly larger error due to their lower occupancies.

IV. DISCUSSION

At this point, it is necessary to find a structural model of the surface which is able to reconcile the result of the analysis of the diffraction data and the STM images. In the STO(103)-(1×2) model of Fig. 5, the atomic occupancies are increasing with depth being very closed to multiples of 1/6. The correlation between this model and the steps structure seen in STM images (Fig. 1) can be explained by a STO(103)-(6×2) superstructure with full atomic occupancy. This is illustrated in Fig. 6(a), where six (103)-(1×2) unit cells along the X direction are shown. The "filling" of the STO(103) unit cells with atoms has been performed in such a way that the occupancies of the cations, when projected back

TABLE I. Ideal position and relative displacements of nonequivalent Sr and Ti atoms in a (1×2) unit cell. The column O_c indicates the occupancy of the corresponding atom. $d_{\text{Ti-O(PE)}}$ and $d_{\text{Ti-O(PA)}}$ are the average bond distances (Å) between Ti and O atoms parallel and perpendicular to the surface for each Ti octahedron. For clarity, we did not give the oxygen positions because they are almost in the bulklike position and relative displacements decrease very fast with depth. The mean relative displacements (normalized values) of oxygen along X, Y, and Z directions in the first four layers are, respectively, −0.054, 0, and −0.024 for the first layer ($\mathbf{Z}/\mathbf{a}_Z\approx0.9$), −0.033, 0, and −0.011 for the second layer ($\mathbf{Z}/\mathbf{a}_Z\approx0.8$), −0.011, 0, and −0.008 for the third layer ($\mathbf{Z}/\mathbf{a}_Z\approx0.7$), −0.007, 0, 0.001 for the fourth layer ($\mathbf{Z}/\mathbf{a}_Z\approx0.6$). The estimated errors for the refined atomic displacements (ΔX, ΔY, ΔZ) and occupancy ($\boldsymbol{\Delta}\ O_c$) are (±0.003, ±0.003, ±0.004) and (±0.03), respectively.

Atom	$\mathbf{X}/\mathbf{a}_X$		$\mathbf{Y}/\mathbf{a}_Y$		$\mathbf{Z}/\mathbf{a}_Z$		O_c	$d_{\text{Ti-O(PE)}}$	$d_{\text{Ti-O(PA)}}$
Sr_1	2/10	(−0.044)	1/4	(−0.014)	9/10	(+0.028)	0.11		
Sr_2	9/10	(−0.014)	1/4	(+0.010)	8/10	(+0.002)	0.24		
Sr_3	6/10	(+0.003)	1/4	(+0.021)	7/10	(+0.003)	0.48		
Sr_4	3/10	(−0.010)	1/4	(−0.010)	6/10	(+0.002)	0.69		
Sr_5	0	(−0.003)	1/4	(+0.014)	1/2	(+0.000)	0.89		
Sr_6	7/10	(−0.009)	1/4	(+0.007)	4/10	(+0.002)	0.95		
Sr_7	4/10	(+0.003)	1/4	(−0.004)	3/10	(−0.002)	1.00		
Sr_8	1/10	(−0.004)	1/4	(−0.003)	2/10	(+0.001)	1.00		
Sr_9	8/10	(+0.003)	1/4	(+0.000)	1/10	(−0.001)	1.00		
Sr_{10}	1/2	(−0.001)	1/4	(+0.001)	0	(−0.001)	1.00		
Ti_1	7/10	(−0.023)	0		9/10	(+0.037)	0.18	2.2	2.1
Ti_2	7/10	(−0.023)	1/2		9/10	(+0.037)	0.18	2.2	1.9
Ti_3	4/10	(−0.037)	0		8/10	(+0.018)	0.32	1.7	1.8
Ti_4	4/10	(−0.043)	1/2		8/10	(+0.008)	0.32	1.7	2.0
Ti_5	1/10	(+0.020)	0		7/10	(−0.021)	0.50	2.1	1.9
Ti_6	1/10	(−0.046)	1/2		7/10	(+0.015)	0.50	2.2	2.0
Ti_7	8/10	(+0.000)	0		6/10	(−0.002)	0.63	2.0	1.9
Ti_8	8/10	(−0.018)	1/2		6/10	(−0.018)	0.63	1.7	2.0
Ti_9	1/2	(+0.018)	0		1/2	(+0.001)	0.82	2.3	1.9
Ti_{10}	1/2	(−0.013)	1/2		1/2	(−0.015)	0.82	2.2	1.9
Ti_{11}	2/10	(+0.016)	0		4/10	(+0.001)	1.00	1.9	1.9
Ti_{12}	2/10	(−0.020)	1/2		4/10	(−0.014)	1.00	1.7	2.1
Ti_{13}	9/10	(+0.000)	0		3/10	(−0.006)	1.00		
Ti_{14}	9/10	(+0.001)	1/2		3/10	(−0.009)	1.00		
Ti_{15}	6/10	(+0.004)	0		2/10	(−0.004)	1.00		
Ti_{16}	6/10	(−0.003)	1/2		2/10	(−0.005)	1.00		
Ti_{17}	3/10	(+0.001)	0		1/10	(−0.006)	1.00		
Ti_{18}	3/10	(+0.000)	1/2		1/10	(−0.001)	1.00		
Ti_{19}	0	(+0.000)	0		0	(−0.005)	1.00		
Ti_{20}	0	(−0.001)	1/2		0	(+0.001)	1.00		

into a single STO(103)-(1×2) unit cell, follow a linear dependence on their Z-coordinate according to the values in Table I. This means that along the X direction, atoms are simply gradually missing, resulting in a 7.5 nm wide terrace or facet, which is by about 6 degrees inclined with respect to the ideal (103) surface. The resulting ordered superstructure resembles well the STM image in Fig. 6(b) which show a corresponding ridge-valley periodicity and terraces inclined with respect to the (103) surface. As observed in the STM images in Fig. 1(b), the period of the wavy shaped surface along the [100] direction is not always constant. However, the averaged period observed along this direction corresponds to six STO(103) surface unit cells. The slope of the facets is closer to a (102) face than to the (103). This would explain the presence of one reflection instead of two between the $3*n$ reflections in the LEED pattern in Fig. 1.

The model shown in Fig. 6(a) suggests that the surface of this STO(103)-6×2 supercell is neutrally charged since the topmost surface layer is Sr and Ti terminated. In fact, by dividing the 6-STO(103) unit cells in individual cells from 1 to 6, we can observe that unit cells 3 and 6 are Sr terminated while unit cells 1 and 5 are Ti terminated in the same proportion as the Sr-terminated cells. The others cells (2 and 4) are equally Sr and Ti terminated. Thus, the charge distribution in the supercell is neutral as in the case of the STO(106) stepped surface.[13]

The refinement done for the (1×2) supercell indicates significant lateral as well as out-of-plane relaxations. More specifically, the refinement of the structural parameters of the oxygen atoms shows that there are O atoms on top of the topmost Ti (but not on the Sr) surface atoms, forming closed octahedral units (Fig. 5). The cation/O ratios for the topmost (Ti-Sr)O_x surface layer are about $Ti_1/O \approx 1/3$ and $Sr_1/O \approx 1/2$. The Ti and Sr oxygen ratios of deeper layers are close to their respective bulk values of 1/2 and 1, respectively, which is in agreement with the charge neutrality required by the calculated Bader's topological charges ($q_{Ti}=+2.18$, $q_O=-1.26$, and $q_{Sr}=1.58$).[19] The average atomic displacements of the oxygen atoms in the surface cell are similar to those of the metal atoms. The average Ti-O bond distances of the octahedral units are given for Ti_1 to Ti_{12} atoms in Table I, where the distances are averaged over the four Ti-O bonds parallel ($d_{Ti\text{-}O(PA)}$) and the twoTi-O bonds perpendicular ($d_{Ti\text{-}O(PE)}$) to the surface. The maximum depth from the surface of the empty region deduced from Fig. 6(a) is of about 0.8 nm, which is in quite good agreement with the maximum corrugation observed in the STM profile [Fig. 6(b)].

V. CONCLUSION

To conclude, the surface of STO(103) shows regular facets with an averaged periodicity of six (103) unit cells in the *X* direction instead of a (103) surface formed simply by (100) terraces. This results in a periodic ripple structure comparable to the structure of STO(106). The main difference with the (106) surface is, however, that there is no alternating TiO_2 and SrO surface termination caused by half-steps. Furthermore, on the (103) surface, two length scales are involved in forming the resulting surface structure. These characteristic differences with the (106) surface may be well caused by the fact that alternating Sr and Ti terminations of the (103) surface by (001) terraces separated by half-steps may energetically not be favorable because of its odd character. A way to support this assumption is to investigate other vicinal surfaces such as (104) and (105). Another interesting feature about the facetted (103) surface is that the slope of each facet is closer to a STO(102) surface, i.e., an "even" surface, rather than to the (103) surface. This observation is confirmed by the LEED pattern shown on Fig. 1(a) which exhibits additional spots in the *h* direction. These spots due to CTRs are located at intermediate positions between $3n/2$ and $2n$.

*Electronic address: isabelle.joumard@esrf.fr

[1] J. F. Schooley, W. R. Hosler, and M. L. Cohen, Phys. Rev. Lett. **12**, 474 (1964).
[2] J. G. Mavroides, J. A. Kafalas, and D. F. Kolesar, Appl. Phys. Lett. **28**, 241 (1976).
[3] V. Ravikumar, D. Wolf, and V. P. Dravid, Phys. Rev. Lett. **74**, 960 (1995).
[4] T. Bieger, J. Maier, and R. Waser, Sens. Actuators B **7**, 763 (1992).
[5] R. A. McKee, F. J. Walker, and M. F. Chisholm, Phys. Rev. Lett. **81**, 3014 (1998).
[6] K. Eisenbeiser, J. M. Finder, Z. Yu, J. Ramdani, J. A. Curless, J. A. Hallmark, R. Droopad, W. J. Ooms, L. Salem, S. Bradshaw, and C. D. Overgaard, Appl. Phys. Lett. **76**, 1324 (2000).
[7] R. von Helmolt, J. Wecker, B. Holzapfel, L. Schultz, and K. Samwer, Phys. Rev. Lett. **71**, 2331 (1993).
[8] See, e.g., J. Zegenhagen, T. Haage, and Q. D. Jiang, Appl. Phys. A: Mater. Sci. Process. **67**, 711 (1998).
[9] C. Jooss, R. Warthmann, H. Kronmüller, T. Haage, H.-U. Habermeier, and J. Zegenhagen, Phys. Rev. Lett. **82**, 632 (1999).
[10] N. Erdman, K. R. Poeppelmeier, M. Asta, O. Warschkow, D. E. Ellis, and L. D. Marks, Nature (London) **419**, 55 (2002).
[11] J. Brunen and J. Zegenhagen, Surf. Sci. **389**, 349 (1997), and references therein.
[12] C. Noguera, J. Phys.: Condens. Matter **12**, R367 (2000).
[13] X. Torrelles, J. Zegenhagen, J. Rius, T. Gloege, L. X. Cao, and W. Moritz, Surf. Sci. **589**, 184 (2005).
[14] Y. Liang and D. A. Bonnell, Surf. Sci. **285**, L510 (1993).
[15] Q. D. Jiang and J. Zegenhagen, Surf. Sci. **425**, 343 (1999).
[16] M. R. Castell, Surf. Sci. **505**, 1 (2002).
[17] T. Haage, J. Zegenhagen, J. Q. Li, H.-U. Habermeier, M. Cardona, C. Jooss, R. Warthmann, A. Forkl, and H. Kronmüller, Phys. Rev. B **56**, 8404 (1997).
[18] E. Vlieg, J. Appl. Crystallogr. **33**, 401 (2000).
[19] F. Bottin, F. Finocchi, and C. Noguera, Phys. Rev. B **68**, 035418 (2003).